Influence of Blast Directionality, Intensity, and Combat Helmet Use on Head Surface Pressure Responses

A. J. Nelson[1], E. T. Burt[1], J. M. Hamilton[2], K. J. Espinoza[2],
J. Magallanes[2], and P. J. VandeVord[1]
[1] Department of Biomedical Engineering, Virginia Tech; [2] Karagozian & Case Inc.

ABSTRACT

The widespread use of explosive weapons in recent military conflicts has contributed to an increased incidence of traumatic brain injuries. Although current infantry helmets provide effective protection against fragmentation, ballistic impact, and blunt trauma, they are not designed to mitigate primary blast loading. Previous studies suggest that blast waves may infiltrate the space between the head and helmet, leading to localized increases in pressure on the head surface, a phenomenon referred to as the underwash effect. However, experimental validation of the underwash effect remains limited, particularly for blast scenarios representative of buried-charge detonations, despite their potential to increase underwash-related loading across large regions of the cranial surface. This study experimentally evaluated the effects of combat helmet use, blast orientation, and blast intensity on head surface loading to assess helmet protective performance across various blast scenarios. A human surrogate headform instrumented with four flush-mounted pressure sensors was exposed to blast overpressures of approximately 16 and 24 psi using a large advanced blast simulator. Tests were conducted at 0° and 45° head orientations (rotation about the transverse axis), both with and without a combat helmet, with three repetitions per combination of experimental conditions. In the 0° orientation, helmet use reduced loading at the forehead and anterior head but increased loading at the posterior region. In the 45° orientation, helmet use led to increased peak pressure and total impulse at all measured locations. Increasing the blast intensity resulted in similar trends for both orientations and helmet conditions but with greater peak pressures and total impulses at each measured location. These findings suggest that certain blast orientations exacerbate the underwash effect and amplify cranial loading beneath the helmet. This work advances understanding of orientation-dependent blast loading, highlights limitations in current helmet performance, and offers guidance to support the development of future protective technologies.

INTRODUCTION

The use of explosive weapons in military conflicts has increased over the past century, resulting in a corresponding rise in traumatic brain injuries (TBIs). More than 530,000 U.S. military service members have been diagnosed with a TBI since the year 2000, and blast events were found to be the most common cause of TBI among these service members during the Iraq

This paper is a student paper from the 21st Injury Biomechanics Symposium and is published in a special issue of SAE International Journal of Transportation Safety.
It is preliminary work, has not been peer reviewed, and should not be cited because it is a work in progress.

and Afghanistan war era (Traumatic Brain Injury Center of Excellence (TBICoE), 2026, Lindquist et al., 2017). Consequently, the high prevalence of blast traumatic brain injuries (bTBIs) in these conflicts has brought renewed attention to the effectiveness of combat helmets in mitigating blast-related injuries.

The primary function of a combat helmet is to reduce the risk of head injury during combat or operational activities. Early combat helmet designs were intended to protect against head injury caused by swords and blunt trauma. During World War I and World War II, the combat helmet evolved to provide protection against shell fragments and shrapnel, although they lacked ballistic resistance (National Research Council, 2014). In more recent conflicts, such as Operation Iraqi Freedom and Operation Enduring Freedom, helmets such as the advanced combat helmet (ACH) were developed to offer ballistic, fragmentation, and impact protection. Subsequent designs, including the enhanced combat helmet (ECH) and the Integrated Head Protection System (IHPS), further improved upon the ballistic, fragmentation, and impact protection; however, no current field infantry combat helmet has been specifically designed to protect against blast exposure (National Research Council, 2014). While the nature of battlefield threats has evolved, the fundamental purpose has remained the same: to protect the wearer's head from injury (Wallace and Rayner, 2012). As more is known about the physiological and psychological consequences of bTBI, there is a need for protective systems that address not only ballistics, impact, projectiles, and shrapnel but also primary blast exposure. The National Research Council has recommended that the U.S. Department of Defense develop helmet testing metrics that specifically account for blast-related injury mechanisms; however, such protocols have yet to be established, largely due to the absence of a well-defined dose-response relationship for blast exposure that reliably translates to human injury (National Research Council, 2014).

Previous work has shown that the ACH provides minimal improvements in blast protection compared to historical helmets used in World War I when evaluated under overhead blast conditions (Op 't Eynde et al., 2020). In 2008, Mott et al. first described the phenomenon later coined as the underwash effect, in which a blast wave infiltrates the gap between the head and helmet, generating localized regions of increased pressure on the surface of the head (Moss et al., 2009, Mott et al., 2008). This amplified pressure typically occurs on the side of the head opposite the blast source. The mechanism responsible for the underwash effect remains a topic of debate. The amplified pressure has been attributed to geometric focusing of the shock wave in the helmet-head gap (Moss et al., 2009). It has also been postulated that the shock wave external to the helmet propagates more rapidly than the flow within the helmet gap, leading to flow blockage at the rear of the helmet and the subsequent formation of a high-pressure region (Sarvghad-Moghaddam et al., 2017). Furthermore, it has been suggested that a collision of the shock wave outside the helmet with the shock wave inside the helmet contributes to the observed pressure amplifications (Li et al., 2020). While the underwash effect has been reproduced with various computational models, experimental validation of these findings remains limited (Li et al., 2020, Thomas and Johnson, 2024, Zhang et al., 2024, Santhanam and Alagappan, 2024).

Both experimental and computational studies have examined the effect of head orientation on blast loading, with most work focusing on frontal exposures or rotations about the longitudinal axis, e.g. side and back (Skotak et al., 2020, Sarvghad-Moghaddam et al., 2017, Thomas and Johnson, 2024). These studies demonstrate that head orientation relative to the blast wave

This paper is a student paper from the 21st Injury Biomechanics Symposium and is published in a special issue of SAE International Journal of Transportation Safety.
It is preliminary work, has not been peer reviewed, and should not be cited because it is a work in progress.

significantly affects surface pressure distributions, with peak overpressures occurring on both the side of the head facing the blast wave and the opposite side; however, the effect of a blast originating from an anterior-inferior position on loading at the head surface has not been previously evaluated. Given that the underwash-related loading has been suggested to occur on the side opposite of the blast source (Skotak et al., 2020), a configuration in which the head and neck are rotated 45° about the transverse axis, perhaps representative of primary blast exposure from a buried charge, could result in increased loading across a substantial area of the cranial surface.

Therefore, the objective of this study was to experimentally assess the effects of head orientation, blast intensity, and the presence of the combat helmet on blast loading at the head surface. This work aims to advance the understanding of the effectiveness of current protective equipment in blast environments and to inform the design of next-generation combat helmets.

METHODS

Experiment Design

A large advanced blast simulator (ABS4) located at Virginia Tech's Center for Injury Biomechanics (Figure 1A) was used to expose an instrumented human skull surrogate headform to two blast overpressure levels (approximately 16 and 24 psi), in two blast orientations (0° or 45° rotation about the transverse axis), with and without a combat helmet. The ABS4 measures 40 ft in length with a testing cross-section of 4 ft by 4 ft, which allows for proper clearance around the headform and permits the wrap-around loading that develops with real-world blasts (Needham et al., 2015, Norris et al., 2024, Nelson et al., 2024). The instrumented headform was affixed to a stand in the center of the ABS4 test section that allowed for the upright, 0° orientation or the angled, 45° orientation, as shown in Figure 1B. Three tests were conducted for each combination of blast intensity, orientation, and helmet configuration, for a total of 24 blasts. High-speed videos of the blast exposures were collected with a Phantom Miro high-speed camera (Miro eX2, AMETEK, Inc.). Frontal and lateral view images of the headform positioned in the ABS4 in the various blast orientations and helmet configurations are shown in Figure 2. Peak pressure and total impulse were determined to quantify the blast loading on the head. Peak pressure was designated as the absolute maximum positive pressure during the exposure, and total impulse was computed as the integral of the pressure-time profile during the positive overpressure phase.

Figure 1: (A) A lateral view of the ABS4 at Virginia Tech with the mounting location of the headform highlighted and (B) the headform mounted to a stand in the center of the ABS4 test section.

This paper is a student paper from the 21st Injury Biomechanics Symposium and is published in a special issue of SAE International Journal of Transportation Safety.
It is preliminary work, has not been peer reviewed, and should not be cited because it is a work in progress.

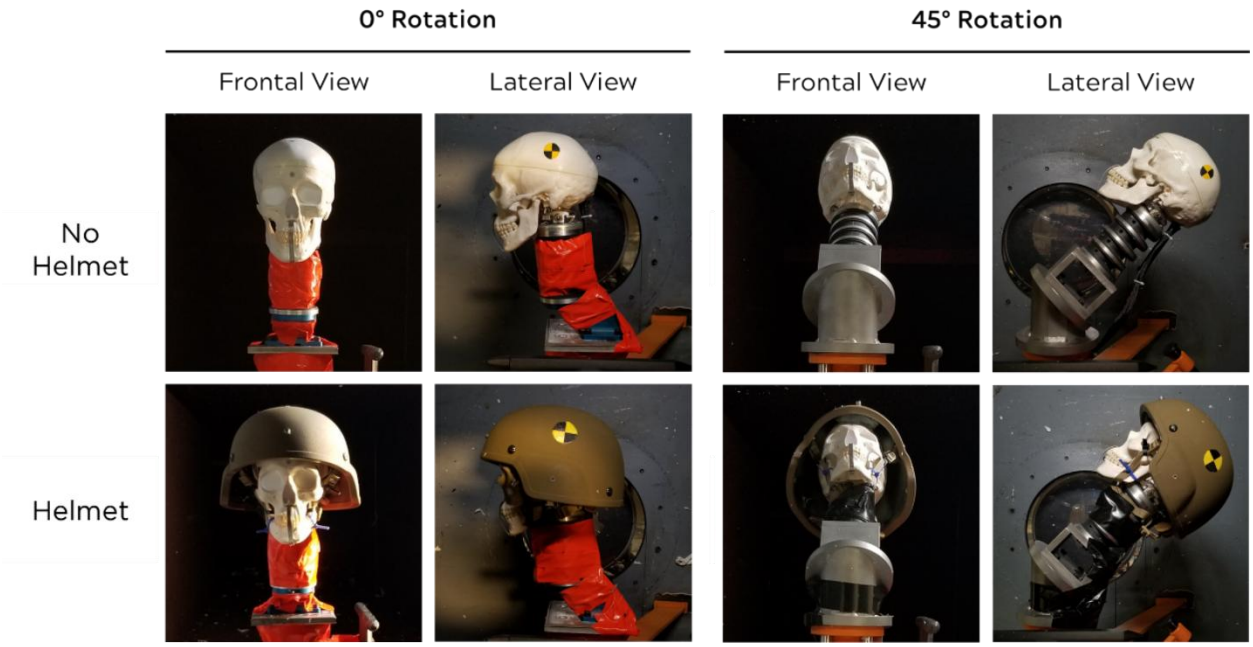

Figure 2: Frontal and lateral photos of the headform mounted in the ABS4 with and without a helmet and in 0° and 45° rotation configurations.

Headform Fabrication and Instrumentation

A synthetic human skull model (3B Scientific, Model 1020159) was affixed to a Hybrid III 50th percentile male neck (Humanetics, Model 78051-218-H) with a fabricated metal upper neck bracket set in a polyurethane resin (Polytek Development Corporation, EasyFlo 60 Liquid Plastic). To prevent the blast wave from entering the skull, the orbits and nasal cavity were also filled with the polyurethane resin. The skull was instrumented with four pressure transducers (Endevco, Model 8540-200) mounted flush with the surface of the skull and facing externally, as illustrated in Figure 3.

Three pressure transducers were placed along the midline, with one in the forehead, one in the top front of the head, and one in the crown of the head. The fourth pressure transducer was placed on the side of the skull superior to the temporal bone. An enhanced combat helmet (ECH) was fastened to the skull with the chin strap and secured with cable ties for the helmeted tests. A seven-pad system was installed inside the combat helmet to replicate standard military helmet configurations.

This paper is a student paper from the 21st Injury Biomechanics Symposium and is published in a special issue of SAE International Journal of Transportation Safety.
It is preliminary work, has not been peer reviewed, and should not be cited because it is a work in progress.

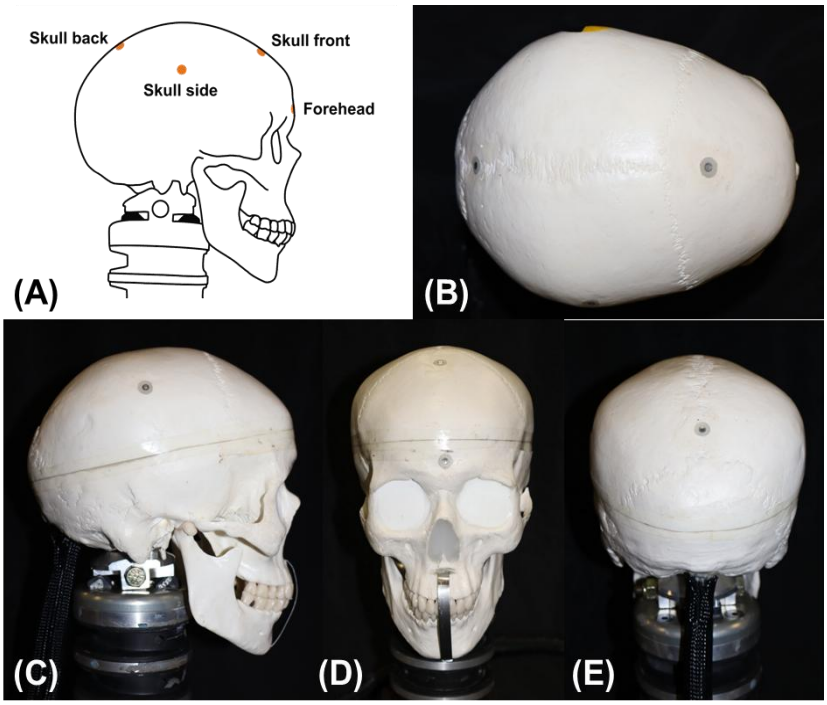

Figure 3: (A) Drawing of the surface-mounted sensor locations and (B) Top, (C) Lateral, (D) Frontal, and (E) Rear views of the instrumented headform.

ABS4 Instrumentation

The overhead wall of the ABS4 test section was instrumented with three flush-mounted pressure transducers (Endevco, Model 8540-200) to measure static overpressure (Figure 4). Wall Sensor 2 was located directly above the mounted headform and Wall Sensors 1 and 3 were located 15.5 inches closer to and further away from the blast source, respectively. A pitot probe was attached to the stand supporting the headform to measure total pressure at the tip (Endevco, Model 8530B-500) and static overpressure along the side (Endevco, Model 8530C-100). All data were conditioned and acquired using a TMX Multi-Channel High Speed Data Acquisition Recorder (AstroNova Inc., Model TMX-18), and signals were sampled at 800 kHz.

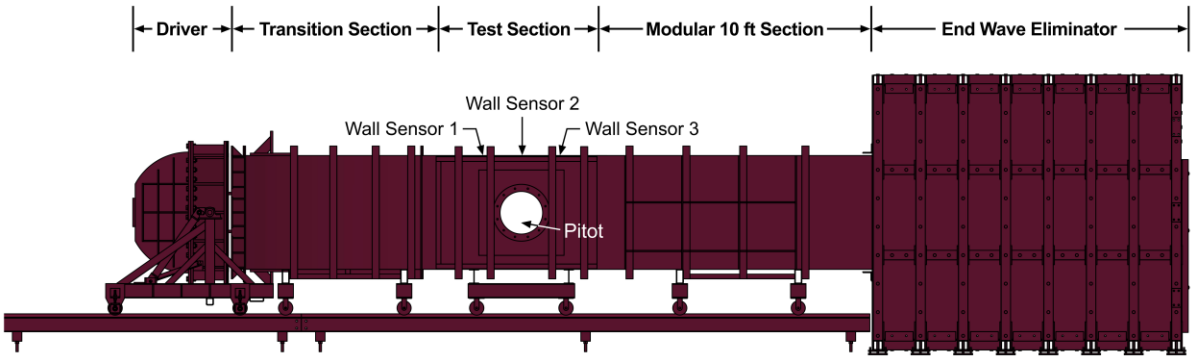

Figure 4: Drawing of a lateral view of the ABS4 labeled with wall sensor and pitot probe sensor locations.

This paper is a student paper from the 21st Injury Biomechanics Symposium and is published in a special issue of SAE International Journal of Transportation Safety.
It is preliminary work, has not been peer reviewed, and should not be cited because it is a work in progress.

RESULTS

Representative pressure-time traces for the ABS4 sensors are shown for the 16 psi and 24 psi target pressure conditions in Figure 5. The propagation of the blast wave through the ABS4 test section is illustrated by the measurements at the wall sensors. The recorded pressure histories indicate that the blast wave arrived simultaneously at both the centrally located pitot side sensor and the Wall 2 sensor mounted above the pitot probe along the chamber wall. This concurrence in arrival time suggests that the blast wave maintained a high degree of planarity as it propagated through the blast chamber. The pitot probe side sensor exhibits an initial peak comparable to that recorded at Wall 2, followed almost immediately by a secondary increase attributed to a reflected wave from the headform mount, consistent with the probe's placement just beneath the mount.

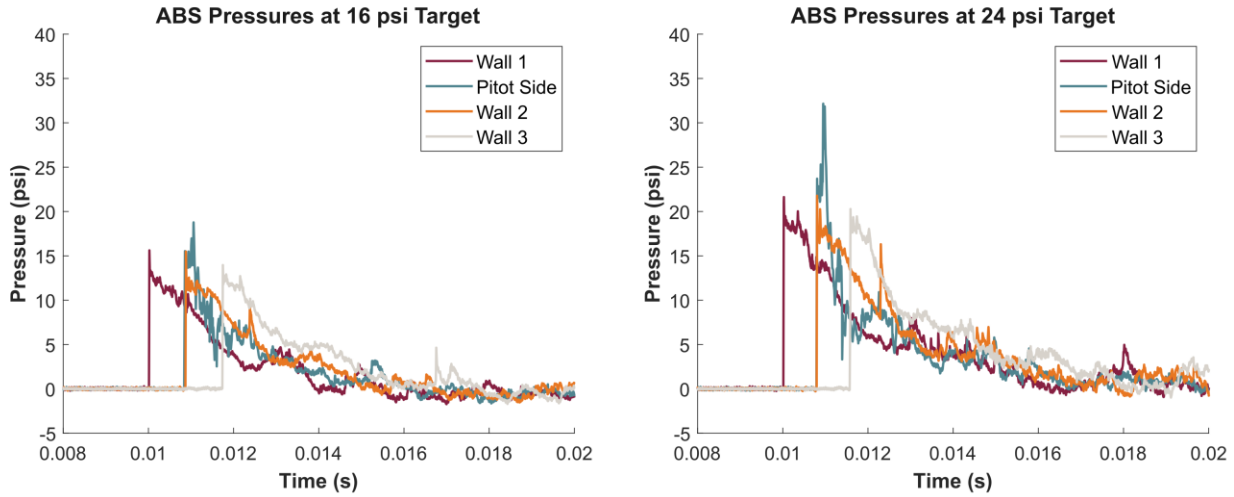

Figure 5: Representative pressure-time profiles as measured by the ABS4 wall and pitot side sensors for a target pressure of 16 psi (left) and 24 psi (right).

Figure 6 depicts representative pressure-time curves recorded by the skull-mounted sensors for each orientation and helmet condition at the 16 psi incident pressure. Corresponding average peak pressures and total impulses for each orientation and helmet condition at the same 16 psi incident pressure are plotted in Figure 7. Representative pressure-time profiles and plots of the corresponding average peak pressures and total impulses for the skull-mounted sensors are presented for the 24 psi incident pressure in Figure 8 and Figure 9, respectively.

This paper is a student paper from the 21st Injury Biomechanics Symposium and is published in a special issue of SAE International Journal of Transportation Safety.
It is preliminary work, has not been peer reviewed, and should not be cited because it is a work in progress.

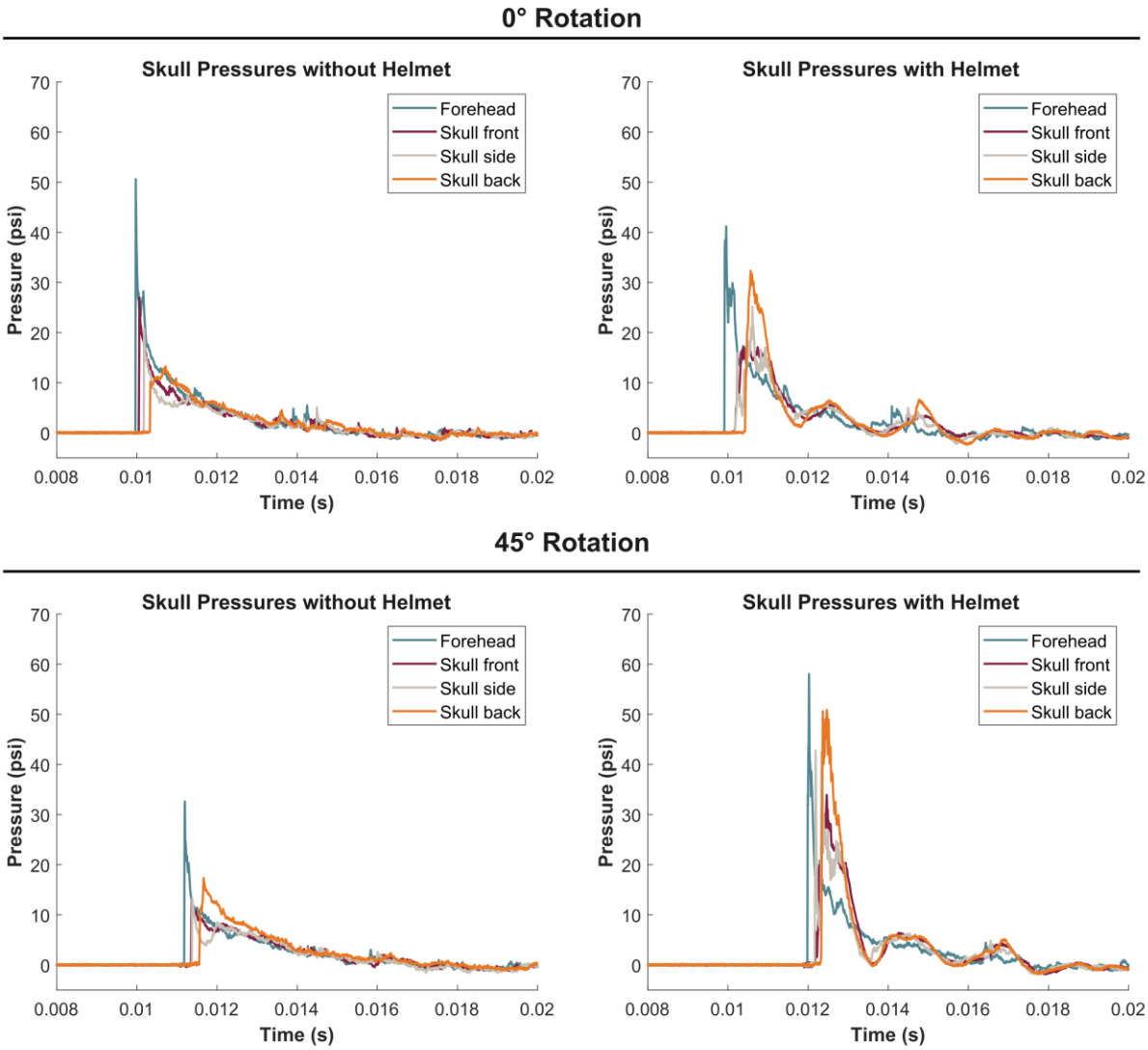

Figure 6: Representative pressure-time traces measured on the skull surface without the helmet (left) and with the helmet (right) and in the 0° rotation orientation (top) and the 45° rotation orientation (bottom) for the 16 psi target incident pressure.

This paper is a student paper from the 21st Injury Biomechanics Symposium and is published in a special issue of SAE International Journal of Transportation Safety.
It is preliminary work, has not been peer reviewed, and should not be cited because it is a work in progress.

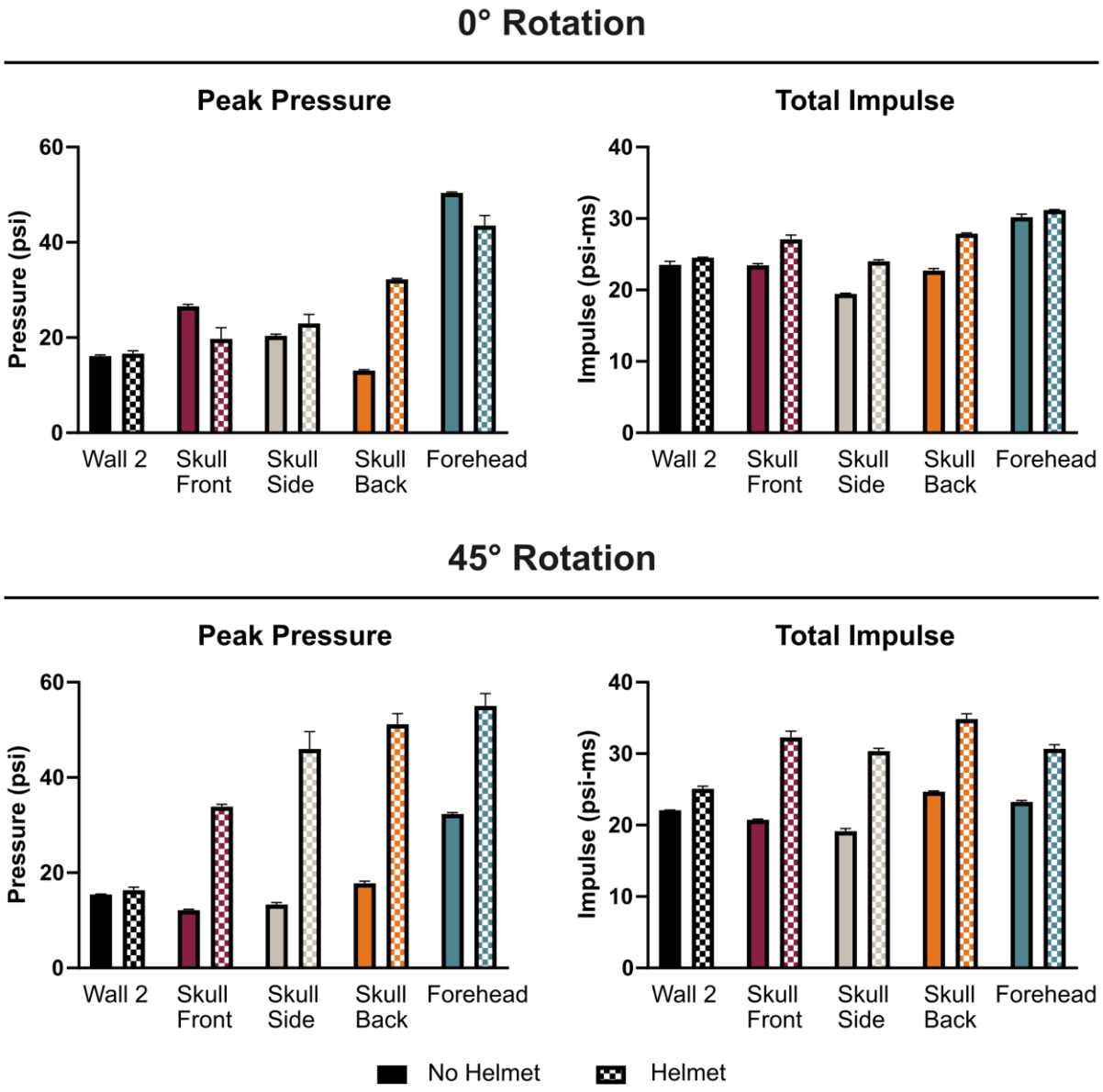

Figure 7: Mean peak pressure (left) and total impulse (right) as measured at various locations on the skull surface and the ABS wall directly above the mounted headform for the 0° rotation (top) and 45° rotation (bottom) orientations at the 16 psi target incident pressure.

This paper is a student paper from the 21st Injury Biomechanics Symposium and is published in a special issue of SAE International Journal of Transportation Safety.
It is preliminary work, has not been peer reviewed, and should not be cited because it is a work in progress.

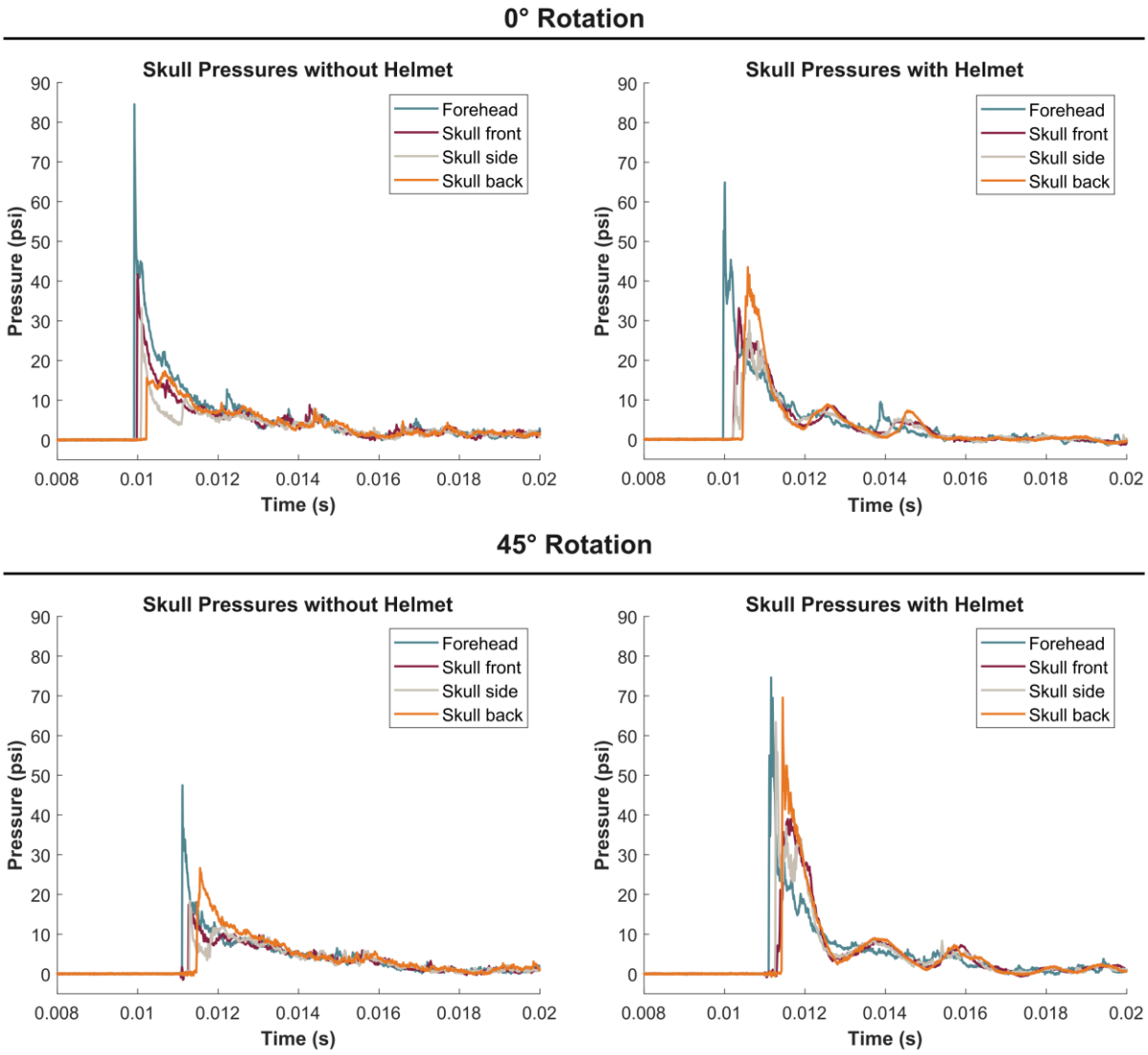

Figure 8: Representative pressure-time traces measured on the skull surface without the helmet (left) and with the helmet (right) and in the 0° rotation orientation (top) and the 45° rotation orientation (bottom) for the 24 psi target incident pressure.

This paper is a student paper from the 21st Injury Biomechanics Symposium and is published in a special issue of SAE International Journal of Transportation Safety.
It is preliminary work, has not been peer reviewed, and should not be cited because it is a work in progress.

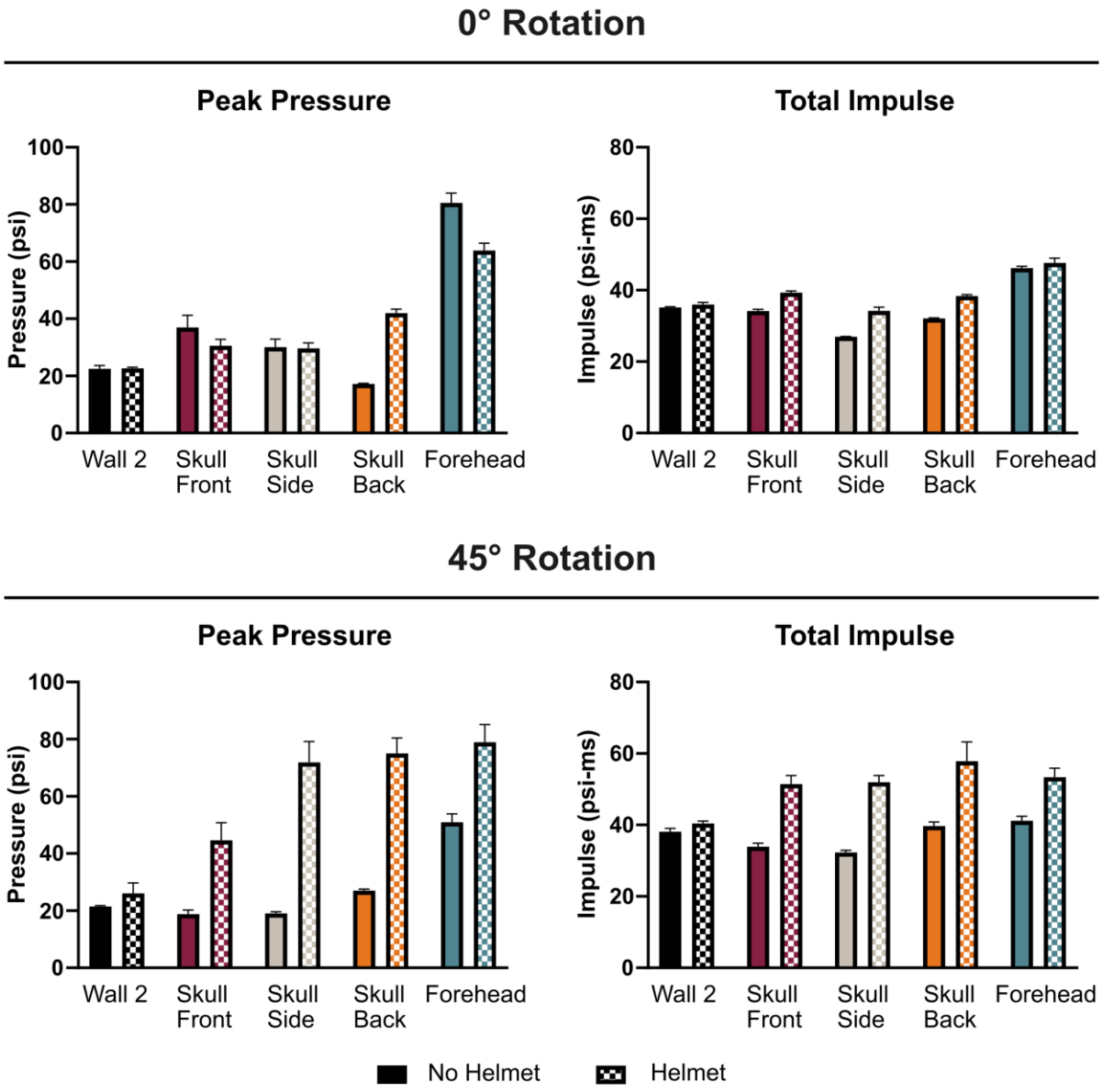

Figure 9: Mean peak pressure (left) and total impulse (right) as measured at various locations on the skull surface and the ABS wall directly above the mounted headform for the 0° rotation (top) and 45° rotation (bottom) orientations at the 24 psi target incident pressure.

Trinitrotoluene (TNT) equivalency is a method for quantifying the strength of an energetic material by expressing it in terms of the mass of TNT required to produce comparable blast effects, providing a standardized basis for testing and comparing different explosives (Jaansalu et al., 2020). OverPressure (version 1.0) software, was employed to back-calculate the equivalent TNT charge weights and corresponding standoff distances for each blast intensity level, using the average measured peak pressure and total impulse values (Jacques, 2018), and an equivalence factor of 1.3 was applied to the TNT charge weight to also estimate the equivalent C-4 charge

This paper is a student paper from the 21st Injury Biomechanics Symposium and is published in a special issue of SAE International Journal of Transportation Safety.
It is preliminary work, has not been peer reviewed, and should not be cited because it is a work in progress.

weight. The average blast parameters, equivalent charge weights, and corresponding standoff distances are provided in Table 1.

Table 1: Blast wave parameters (reported as mean ± standard error of the mean) and calculated equivalent TNT and C-4 charge weights with corresponding standoff distances

Mean Peak Static Pressure (psi)	Mean Total Impulse (psi-ms)	Equivalent TNT Charge Weight (lbs)	Equivalent C-4 Charge Weight (lbs)	Standoff Distance (ft)
16.11 ± 0.18	23.80 ± 0.35	13.0	10.0	18.1
23.14 ± 0.71	37.61 ± 0.64	32.7	25.2	20.8

Increasing blast intensity from 16 psi to 24 psi resulted in greater peak pressures and total impulses at all skull locations for both orientations and helmet conditions. In the 0° orientation without the helmet, peak skull pressures exceeded the incident pressure at all sensor locations except the back of the skull, whereas with the helmet in place, peak pressures were higher than the incident pressure at all locations. In the 0° rotation orientation at both 16 and 24 psi incident pressure, the helmet reduced peak pressures at the skull front and forehead compared with the unhelmeted condition. In contrast, the peak pressure at the back of the skull increased with helmet use, by 146% at 16 psi and 143% at 24 psi incident pressure. Peak pressure was also increased with helmet use at the skull side location in the 0° orientation at 16 psi but was approximately the same with or without the helmet at 24 psi. Total impulse increased at all skull sensor locations with helmet use in the 0° blast orientation at both 16 and 24 psi. In this configuration, the largest increases in impulse occurred at the skull side and back, with a 23% rise at both locations at 16 psi incident pressure and increases of 27% and 19% at the side and back, respectively, at 24 psi incident pressure. In the 0° orientation without the helmet, the pressure-time histories at the forehead, front, and side of the skull resembled an idealized Friedlander waveform, characterized by a rapid, near-instantaneous rise to peak followed by a gradual exponential decay. With the helmet in place, the pressure peak became less abrupt, and the rise time increased across all sensor locations.

In the 45° orientation without a helmet, the peak pressures at the front and side of the skull were lower than the incident pressure, whereas the pressures at the back of the skull and forehead exceeded the incident peak pressure. However, adding the helmet increased the peak pressure above the incident peak pressure at all sensor locations. In the 45° orientation at both 16 and 24 psi, helmet use increased the peak pressures and total impulses at all skull locations. The largest increase in peak pressure with helmet use occurred at the side of the skull in the 45° orientation, with increases of 245% at 16 psi incident pressure and 277% at 24 psi incident pressure. The increase in total impulse with the helmet was greatest at the skull side and skull front with a difference of 58% and 56%, respectively, at 16 psi incident pressure and a difference of 61% and 52%, respectively, at 24 psi incident pressure.

Regardless of blast orientation or intensity, the helmeted configuration produced an oscillatory pressure waveform during the positive-phase pressure decay at the sensors located beneath the helmet (front, side, and back), with a period of approximately 2 ms. This oscillation

This paper is a student paper from the 21st Injury Biomechanics Symposium and is published in a special issue of SAE International Journal of Transportation Safety.
It is preliminary work, has not been peer reviewed, and should not be cited because it is a work in progress.

was absent in all unhelmeted tests and was not detected by the forehead sensor in the helmeted tests, indicating that it occurred only at sensor locations covered by the combat helmet.

DISCUSSION

Blast orientation, intensity, and helmet condition were found to influence the distribution and magnitude of blast loading. With the headform rotated 45° in the transverse plane and no helmet present, peak pressures were lower at the front, side, and forehead sensors, but higher at the back compared with the 0° orientation. When comparing between the 16 and 24 psi tests in any orientation, the 24 psi test consistently resulted in higher peak pressures and total impulses at each skull location. Peak pressures were expected to vary with changes in orientation, and to increase as blast intensity rose from 16 psi to 24 psi, since the measured values depend on both the strength of the blast and the angle of incidence (U.S. Department of Homeland Security, 2011).

In the 0° orientation, helmet use attenuated peak pressures at the forehead and anterior skull while producing a notable increase at the posterior region for both the 16 and 24 psi incident overpressures. This regional increase in pressure is consistent with previous studies assessing the performance of combat helmets during frontal blast exposure (Li et al., 2020, Thomas and Johnson, 2024, Ganpule et al., 2012). Rotation of the headform 45° about the transverse axis resulted in increased peak pressure and total impulse at all sensor locations with combat helmet use. While this specific orientation has not been previously evaluated, previous work suggests that peak pressures tend to occur on both the surface directly facing the blast and on the opposite side due to wave wrapping and reflection effects (Skotak et al., 2020). In the frontal orientation, the face is positioned towards the blast wave, which results in elevated loading at the face and back of the head. However, rotating the head and neck 45° about the transverse axis would lead to a broader distribution of elevated pressures across the cranium when a helmet is present, as indicated in the present study by increased pressures across all sensor locations with helmet use. The observed increases in regional pressure and total impulse with helmet use and rotation about the transverse axis are consistent with an underwash mechanism and suggest that current helmet designs could inadvertently exacerbate localized mechanical loading, which may have important implications for injury risk in military populations.

For pressures measured beneath the helmet, an oscillatory decay profile was observed. This oscillatory behavior could be caused by rapid reflections of the blast wave between the interior surface of the helmet and the exterior surface of the skull, creating a confined wave environment within the sub-helmet space. Importantly, if the frequency of the observed oscillations approaches the natural frequency of the skull or cranial contents, resonance effects could amplify local mechanical loading and further contribute to injury risk. Future work investigating the source and frequency characteristics of this oscillatory phenomenon is warranted to better understand the blast wave dynamics within the sub-helmet environment and their implications for cranial biomechanics.

This work has limitations that should be addressed in future work. The headform used in the experimental configuration has limited biofidelity, as it does not incorporate compliant soft

This paper is a student paper from the 21st Injury Biomechanics Symposium and is published in a special issue of SAE International Journal of Transportation Safety.
It is preliminary work, has not been peer reviewed, and should not be cited because it is a work in progress.

tissues such as the scalp. The absence of these tissues may influence wave reflection characteristics at the surface of the head, although likely only to a modest extent. Addition of soft-tissue-like materials would improve physiological relevance and might reduce reflective waves, particularly within the sub-helmet space. Furthermore, the head and neck complex was evaluated in isolation, without the inclusion of a torso. Prior work has demonstrated that blast wave reflections from the torso can influence pressure distributions at the head and face (Mott et al., 2017). As such, future studies should incorporate a full-body or torso-coupled model to more accurately capture realistic blast-body interactions and their effects on cranial loading. In addition, the helmet fit on the skull model provided a relatively large gap between the head and the helmet. Computational studies have shown that pressure and impulse beneath the helmet are influenced by the gap size (Ganpule et al., 2012, Tan and Matic, 2021), suggesting that future experimental work should validate the effects of this clearance and examine how variations in helmet fitment and padding configuration influence mechanical loading on the head surface.

CONCLUSIONS

This study examined the underwash effect by quantifying the influence of head orientation, blast intensity, and combat helmet use on blast loading at the head surface. Helmet use in the 0° orientation reduced peak pressures at the forehead and anterior regions of the head, but increased pressures at posterior locations. This pressure redistribution became more pronounced at 45° rotation about the transverse axis, where helmet use resulted in elevated peak pressure and total impulse at all measured locations on the head. These findings suggest that certain blast orientations exacerbate the underwash effect, perhaps allowing greater ingress of the blast wave beneath the helmet and amplifying loading across the cranial surface.

While these results highlight limitations in current helmet performance, they also provide a foundation for targeted design improvements. Future efforts should focus on mitigating underwash through optimized helmet geometry, padding configurations, and interface materials that limit wave transmission into the sub-helmet space. Furthermore, future work should investigate the implications of this localized increased loading. The combat helmet appears to induce regions of elevated pressure on the head surface during blast exposure, prompting consideration of how such pressure elevations may contribute to injury. Establishing the physiological consequences of the increased sub-helmet loading, particularly through *in vivo* or clinically-informed models, will be critical for linking mechanical exposure to neurological outcomes. Collectively, this work advances understanding of orientation-dependent blast loading and provides a framework to guide the development of next-generation protective systems.

ACKNOWLEDGEMENTS

This work was supported by the Defense Health Agency under SBIR Phase I Award No. W81XWH21P0116. The opinions and assertions herein are the private views of the authors and are not to be construed as official or as reflecting the views of the Defense Health Agency or the U.S. Department of Defense.

This paper is a student paper from the 21st Injury Biomechanics Symposium and is published in a special issue of SAE International Journal of Transportation Safety.
It is preliminary work, has not been peer reviewed, and should not be cited because it is a work in progress.

REFERENCES

Advanced Combat Helmet (ACH) [Online]. PEO Soldier: U.S. Army Program Executive Office Soldier. Available: https://www.peosoldier.army.mil/Equipment/Equipment-Portfolio/Project-Manager-Soldier-Survivability-Portfolio/Advanced-Combat-Helmet/ [Accessed Oct 2024].

Enhanced Combat Helmet (ECH) [Online]. PEO Soldier: U.S. Army Program Executive Office Soldier. Available: https://www.peosoldier.army.mil/Equipment/Equipment-Portfolio/Project-Manager-Soldier-Survivability-Portfolio/Enhanced-Combat-Helmet/ [Accessed Oct 2024].

Integrated Head Protection System (IHPS) [Online]. PEO Soldier: U.S. Army Program Executive Office Soldier. Available: https://www.peosoldier.army.mil/Equipment/Equipment-Portfolio/Project-Manager-Soldier-Survivability-Portfolio/Integrated-Head-Protection-System/ [Accessed Oct 2024].

GANPULE, S., GU, L., ALAI, A. & CHANDRA, N. 2012. Role of helmet in the mechanics of shock wave propagation under blast loading conditions. *Comput Methods Biomech Biomed Engin,* 15**,** 1233-44.

JAANSALU, K., COLLET, C., BAKER, E. & VAN DER VOORT, M. 2020. *TNT equivalency testing for energetic materials*.

LI, J., MA, T., HUANG, C., HUANG, X., KANG, Y., LONG, Z. & LIU, M. 2020. Protective Mechanism of Helmet Under Far-field Shock Wave. *International Journal of Impact Engineering,* 143**,** 103617.

LINDQUIST, L. K., LOVE, H. C. & ELBOGEN, E. B. 2017. Traumatic Brain Injury in Iraq and Afghanistan Veterans: New Results From a National Random Sample Study. *J Neuropsychiatry Clin Neurosci,* 29**,** 254-259.

MOSS, W. C., KING, M. J. & BLACKMAN, E. G. 2009. Skull flexure from blast waves: a mechanism for brain injury with implications for helmet design. *Phys Rev Lett,* 103**,** 108702.

MOTT, D., SCHWER, D., YOUNG, T., LEVINE, J., DIONNE, J.-P., MAKRIS, A. & HUBLER, G. 2008. Blast-Induced Pressure Fields Beneath a Military Helmet for Non-Lethal Threats.

MOTT, D. R., SCHWER, D. A. & YOUNG, T. R. 2017. Computational Fluid Dynamics Studies of Blast Loading on Helmeted Warfighters. Naval Research Laboratory.

NATIONAL RESEARCH COUNCIL 2014. *Review of Department of Defense Test Protocols for Combat Helmets,* Washington, DC, The National Academies Press.

NEEDHAM, C. E., RITZEL, D., RULE, G. T., WIRI, S. & YOUNG, L. 2015. Blast Testing Issues and TBI: Experimental Models That Lead to Wrong Conclusions. *Front Neurol,* 6**,** 72.

NELSON, A. J., RITZEL, D., SHOWALTER, N., BOPPE, D., RIEGEL, A. & VANDEVORD, P. J. 2024. Characterization of an Advanced Blast Simulator for Investigation of Large Scale Blast Traumatic Brain Injury Studies. *Annals of Biomedical Engineering*.

NORRIS, C., ARNOLD, B., WILKES, J., SQUIBB, C., NELSON, A. J., SCHWENKER, H., MESISCA, J., VOSSENBERG, A. & VANDEVORD, P. J. 2024. Bilayer surrogate brain response under various blast loading conditions. *Shock Waves*.

OP ‘T EYNDE, J., YU, A. W., ECKERSLEY, C. P. & BASS, C. R. 2020. Primary blast wave protection in combat helmet design: A historical comparison between present day and World War I. *PLOS ONE,* 15**,** e0228802.

This paper is a student paper from the 21st Injury Biomechanics Symposium and is published in a special issue of SAE International Journal of Transportation Safety.
It is preliminary work, has not been peer reviewed, and should not be cited because it is a work in progress.

SANTHANAM, S. S. & ALAGAPPAN, P. 2024. Numerical and experimental study of underwash effect and its role in blast-induced traumatic brain injury. *Shock Waves,* 34**,** 609-624.
SARVGHAD-MOGHADDAM, H., REZAEI, A., ZIEJEWSKI, M. & KARAMI, G. 2017. CFD modeling of the underwash effect of military helmets as a possible mechanism for blast-induced traumatic brain injury. *Comput Methods Biomech Biomed Engin,* 20**,** 16-26.
SKOTAK, M., SALIB, J., MISISTIA, A., CARDENAS, A., ALAY, E., CHANDRA, N. & KAMIMORI, G. H. 2020. Factors Contributing to Increased Blast Overpressure Inside Modern Ballistic Helmets. *Applied Sciences,* 10**,** 7193.
TAN, X. G. & MATIC, P. 2021. Optimizing Helmet Pad Placement Using Computational Predicted Injury Pattern to Reduce Mild Traumatic Brain Injury. *Military Medicine,* 186**,** 592-600.
THOMAS, C. J. H. & JOHNSON, C. E. 2024. Investigation into helmet–head shock wave interactions at low overpressures through free-field blasts and schlieren imagery. *Shock Waves,* 34**,** 399-412.
TRAUMATIC BRAIN INJURY CENTER OF EXCELLENCE (TBICOE) 2026. DOD Numbers for Traumatic Brain Injury Worldwide Totals: 2000-2025 Q3. Defense Health Agency.
U.S. DEPARTMENT OF HOMELAND SECURITY 2011. Reference Manual to Mitigate Potential Terrorist Attacks Against Buildings. *In:* SCIENCE AND TECHNOLOGY DIRECTORATE & DIVISION, I. P. A. D. M. (eds.) 2nd ed.
WALLACE, D. & RAYNER, S. 2012. Combat helmets and blast traumatic brain injury. *Journal of Military and Veterans Health,* 20**,** 10-17.
ZHANG, J., DU, Z., WANG, X., KANG, Y., MA, T., ZHUANG, Z. & LIU, Z. 2024. Analyzing the contribution of helmet components to underwash effect under blast load. *Acta Mechanica Sinica,* 40**,** 124011.

This paper is a student paper from the 21st Injury Biomechanics Symposium and is published in a special issue of SAE International Journal of Transportation Safety.
It is preliminary work, has not been peer reviewed, and should not be cited because it is a work in progress.